Article

Immunity

Integrative Analyses of Colorectal Cancer Show Immunoscore Is a Stronger Predictor of Patient Survival Than Microsatellite Instability

Graphical Abstract

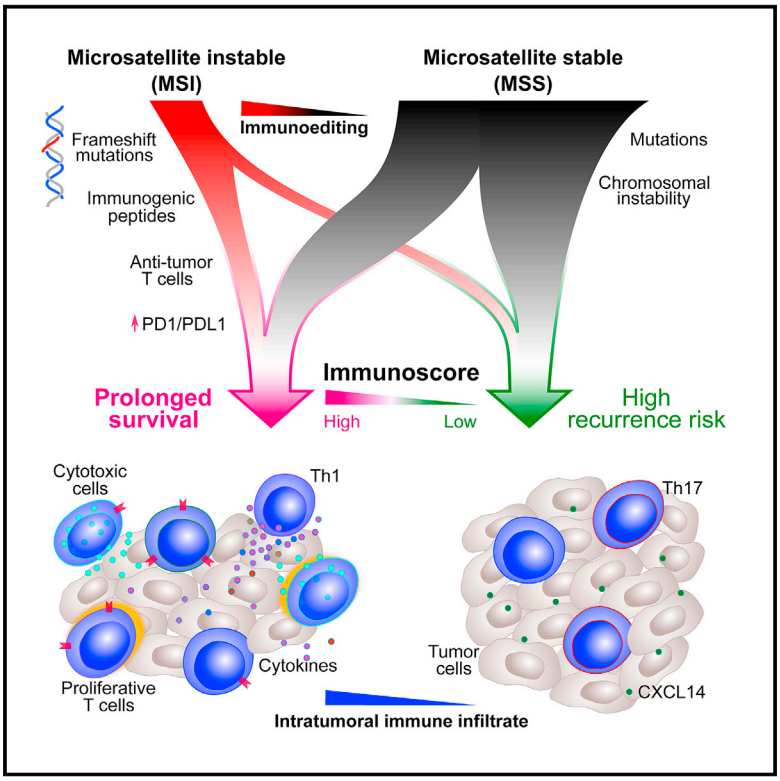

Authors

Bernhard Mlecnik, Gabriela Bindea, Helen K. Angell, ..., Viia Valge-Archer, Jean-Baptiste Latouche, Jérôme Galon

Correspondence

jerome.galon@crc.jussieu.fr

In Brief

Microsatellite instability is due to a DNA mismatch repair deficiency. Galon and colleagues performed a comprehensive analysis of microsatellite-instable tumors and showed the genetic, genomic, and immune landscapes in microsatellite instability. They demonstrated the presence of functional mutation-specific cytotoxic T cells and the superiority of Immunoscore over microsatellite instability in predicting survival.

Highlights

- MSI and a subgroup of MSS patients have high intratumoral adaptive immune gene expression
- Functional effector anti-frameshift mutation CTLs kill tumor cells in MSI patients
- Genetic evidence of immunoediting in human CRC, in particular for MSI patients
- Immunoscore gives an indicator of tumor recurrence and survival beyond MSI staging

Mlecnik et al., 2016, Immunity *44*, 698–711
March 15, 2016
http://dx.doi.org/10.1016/j.immuni.2016.02.025

CellPress

CellPress

Immunity
Article

Integrative Analyses of Colorectal Cancer Show Immunoscore Is a Stronger Predictor of Patient Survival Than Microsatellite Instability

Bernhard Mlecnik,[1,2,3,19] Gabriela Bindea,[1,2,3,19] Helen K. Angell,[1,2,3,4] Pauline Maby,[1,2,3,5] Mihaela Angelova,[1,2,3,6] David Tougeron,[5,7,8] Sarah E. Church,[1,2,3] Lucie Lafontaine,[1,2,3] Maria Fischer,[6] Tessa Fredriksen,[1,2,3] Maristella Sasso,[1,2,3] Amélie M. Bilocq,[1,2,3] Amos Kirilovsky,[1,2,3] Anna C. Obenauf,[9] Mohamad Hamieh,[5] Anne Berger,[1,10] Patrick Bruneval,[11] Jean-Jacques Tuech,[12] Jean-Christophe Sabourin,[13] Florence Le Pessot,[13] Jacques Mauillon,[13,14] Arash Rafii,[15] Pierre Laurent-Puig,[2,16] Michael R. Speicher,[9] Zlatko Trajanoski,[6] Pierre Michel,[7] Richard Sesboüe,[5] Thierry Frebourg,[5,16] Franck Pagès,[1,2,3,17] Viia Valge-Archer,[4,18] Jean-Baptiste Latouche,[5,8] and Jérôme Galon[1,2,3,*]

[1]INSERM, UMRS1138, Laboratory of Integrative Cancer Immunology, 75006 Paris, France
[2]UMRS1138, Université Paris Descartes – Sorbonne Paris Cité, 75006 Paris, France
[3]UMRS1138, Pierre and Marie Curie University (Paris 6) – Sorbonne Paris Cité, Centre de Recherche des Cordeliers, 75006 Paris, France
[4]Innovative Medicines and Early Development, Oncology, AstraZeneca, CB4 OWG Cambridge, UK
[5]INSERM, U1079, Faculté de Médecine, Université de Rouen and the Institute for Research and Innovation in Biomedecine (IRIB), 76000 Rouen, France
[6]Biocenter, Division of Bioinformatics, Innsbruck Medical University, 6020 Innsbruck, Austria
[7]Department of Gastroenterology, Rouen University Hospital, 76000 Rouen, France
[8]Department of Genetics, Rouen University Hospital, 76000 Rouen, France
[9]Institute of Human Genetics, Medical University of Graz, 8010 Graz, Austria
[10]Department of General and Digestive Surgery, Hôpital Européen Georges-Pompidou, Assistance Publique-Hopitaux de Paris, 75015 Paris, France
[11]Department of Anatomopathology, Hôpital Européen Georges-Pompidou, Assistance Publique-Hopitaux de Paris, 75015 Paris, France
[12]Department of Digestive Surgery, Rouen University Hospital, 76000 Rouen, France
[13]Department of Anatomopathology, Rouen University Hospital, 76000 Rouen, France
[14]Department of Gastroenterology, Le Havre Hospital, 76600 Le Havre, France
[15]Stem Cell and Microenvironment Laboratory, Weill Cornell Medical College in Qatar, Education City, Qatar Foundation, 3263 Doha, Qatar
[16]INSERM, UMRS775, Bases Moléculaires de la Réponse aux Xénobiotiques, 75006 Paris, France
[17]Department of Immunology, Hôpital Européen Georges-Pompidou, Assistance Publique-Hopitaux de Paris, 75015 Paris, France
[18]MedImmune, CB21 GGH Cambridge, UK
[19]Co-first author
*Correspondence: jerome.galon@crc.jussieu.fr
http://dx.doi.org/10.1016/j.immuni.2016.02.025

SUMMARY

Microsatellite instability in colorectal cancer predicts favorable outcomes. However, the mechanistic relationship between microsatellite instability, tumor-infiltrating immune cells, Immunoscore, and their impact on patient survival remains to be elucidated. We found significant differences in mutational patterns, chromosomal instability, and gene expression that correlated with patient microsatellite instability status. A prominent immune gene expression was observed in microsatellite-instable (MSI) tumors, as well as in a subgroup of microsatellite-stable (MSS) tumors. MSI tumors had increased frameshift mutations, showed genetic evidence of immunoediting, had higher densities of Th1, effector-memory T cells, in situ proliferating T cells, and inhibitory PD1-PDL1 cells, had high Immunoscores, and were infiltrated with mutation-specific cytotoxic T cells. Multivariate analysis revealed that Immunoscore was superior to microsatellite instability in predicting patients' disease-specific recurrence and survival. These findings indicate that assessment of the immune status via Immunoscore provides a potent indicator of tumor recurrence beyond microsatellite-instability staging that could be an important guide for immunotherapy strategies.

INTRODUCTION

Accumulating evidence suggests that tumor progression and recurrence are governed not only by genetic changes intrinsic to cancer cells, but also by environmental factors (Galon et al., 2014). The American Joint Committee on Cancer (AJCC) and the Union for Internation Cancer Control (UICC) TNM classification has been shown to be valuable in estimating the outcome of patients for a variety of cancers (Locker et al., 2006; Sobin and Wittekind, 2002; Weitz et al., 2005). This approach is powerful, but it provides incomplete prognostic information, given that clinical outcome can vary substantially among patients within the same histological tumor stage (Nagtegaal et al., 2012). A molecular classification of colorectal cancer (CRC) is also used

(Cancer Genome Atlas, 2012), in particular to characterize the group of patients with microsatellite-instable (MSI) tumors. Microsatellite instability in CRC is reported to predict favorable outcome and decreased likelihood of metastases (Gryfe et al., 2000). In CRC, microsatellite instability is due to a DNA mismatch repair (MMR) system deficiency caused by an epigenetic silencing of *MLH1* (a MMR-associated gene) or by germline mutations of a DNA repair gene followed by the somatic inactivation of the second allele (known as Lynch syndrome). This defect leads to accumulation of insertions and deletions in DNA repeat sequences. Furthermore, in genes containing coding repeats, frameshift mutations are a potential source of immunogenic neo-antigens recognized by the immune system (Williams et al., 2010).

The prognostic impact of in situ immune cell infiltrate in tumors has been extensively reported (Atreya and Neurath, 2008; Bindea et al., 2013b; Broussard and Disis, 2011; Finn, 2008; Fridman et al., 2012; Galon et al., 2006; Mlecnik et al., 2011; Pagès et al., 2005; Pagès et al., 2009). Large studies analyzing microsatellite stable (MSS) patients have shown association of T cell subpopulations with prognosis (Nosho et al., 2010; Ogino et al., 2009; Zlobec et al., 2010). "Immunoscore" is a scoring system, based on the quantification of cytotoxic and memory T cells in the core of the tumor (CT) and in the tumor's invasive margin (IM) (Angell and Galon, 2013; Berghoff et al., 2016; Galon et al., 2012a; Galon et al., 2014). Immunoscore is a clinically useful prognostic marker in CRC (Galon et al., 2006; Galon et al., 2012b; Mlecnik et al., 2011; Pagès et al., 2009) and has a dual advantage over TNM staging. First, Immunoscore appears to be the strongest prognostic factor for survival (Galon et al., 2013; Galon et al., 2006; Mlecnik et al., 2011; Pagès et al., 2009), and second, the antitumor activity of these naturally infiltrating T cells might be amenable to enhancement by novel immunotherapy approaches (Brahmer et al., 2012; Des Guetz et al., 2009; Hodi et al., 2010; Robert et al., 2011; Topalian et al., 2012). A pre-existing anti-tumor immune response in the patient is reported to be important in the setting of PD1 blockade (Pardoll, 2012). Therefore, MSI tumors could be more responsive to such treatment (Le et al., 2015), given that they have increased numbers of mutations and neoantigens, a dense immune infiltration (Le et al., 2015), and high amounts of immune checkpoint molecules (Llosa et al., 2015).

Despite previous study, there has been no integrated evaluation of the genetic and genomic changes, the immune patterns in the tumor microenvironment, and their prognostic significance for CRC patients with or without microsatellite instability. Little is also known about the activity and specificity of tumor-infiltrating T cells. Here, we aimed to characterize the existence of anti-tumor T cells within CRC tumors, in relation to tumor genotype, instability status, and immune response. We studied the parameters associated with DNA MMR defects in two cohorts of CRC patients. Mutation patterns, chromosomal instability (CIN) status, and RNA sequencing (RNA-seq) data from 270 patients were analyzed (from the Cancer Genome Atlas [TCGA] cohort), and findings were validated in an independent cohort of 689 patients. Cohort 3 represents all solid tumors from TCGA (n = 3,659). All data were then analyzed in relation to the degree of microsatellite instability. We further investigated the dependency or independency of microsatellite instability and Immunoscore in relation to patient survival.

We demonstrated that immune infiltration and Immunoscore are better at defining the prognosis of CRC patients and identifying patients at high-risk of tumor recurrence, regardless of microsatellite instability.

RESULTS

MSI, and a Subgroup of MSS, Patients Have High Intratumoral Immune Gene Expression and Prolonged Survival

Publicly available RNA-seq data, genomic alterations, and manually curated mutations from 270 CRC patients (cohort 1) (Cancer Genome Atlas, 2012) were compared between MSI patients and the remaining patients in the cohort (MSS) with ClueGO and CluePedia Cytoscape apps (Bindea et al., 2013a; Bindea et al., 2009) developed in our laboratory (Figures 1A and S1A). As previously demonstrated, the MSI group included more patients with hypermutations and *MLH1* silencing patterns than the MSS group did (Figure S1A) and was associated with significantly fewer chromosomal gains and losses (Trautmann et al., 2006). Recurrent somatic mutations in genes including *ACVR2A*, *TGFBR2*, *FBXW7*, and *ARID1A* were observed more frequently in MSI tumors, whereas *APC*, *TP53*, and *KRAS* were less frequently mutated than they were in MSS tumors. A similar profile of genomic aberrations was found in cohort 2 (Figures S1B–S1D). Eleven microsatellite loci (including the new Bethesda panel) were tested in cohort 2 to determine the microsatellite status. CRC patients showed a diverse pattern of instability, some with instability in all markers and others with a single unstable locus (Figure S1E). This analysis, done by unsupervised hierarchical clustering of mutational data, revealed six patient clusters that had no difference in overall survival (OS) (Figure S1F). Similarly, CIN-based groups had a similar OS (Figure S1G). MSI tumors from cohort 1 had 456 upregulated (Hi cluster) and 495 downregulated (Lo cluster) genes in comparison to MSS tumors (Figure 1A). The unsupervised hierarchical clustering of the expression data showed that most of the MSI patient samples had a similar profile and clustered together. In comparison, the MSS samples showed a more heterogeneous pattern. These 951 differentially regulated genes were mainly associated with immune-related functions, encompassing antigen processing and presentation, interferon-gamma signaling, response to cytokines, leukocyte migration, viral processes, and response to tumor-necrosis-factor-related pathways (Figure 1B). The genes that were most highly expressed in MSI tumors were primarily associated with these immune pathways (Figure 1C). Despite similar gene cluster size, and after application of identical pathway selection criteria, the translational initiation function was the only pathway associated with the Lo-cluster of downregulated genes.

Additionally, the immunome, a compendium of 28 immune cell types infiltrating tumors (Bindea et al., 2014; Bindea et al., 2013b), was analyzed in MSI and MSS patients from cohort 1, and known T helper 1 (Th1)-related genes, cytokines, and cytokine receptors were evaluated. Of all immune subpopulations, cytotoxic, CD8, Th1, Th2, T follicular helper (Tfh), and T cell markers had significantly higher expression in MSI than in MSS tumors (Figure 2A). One marker for each of the subtypes—dendritic cells, activated dendritic cells, macrophages, and neutrophils—was included in the network of differentially expressed

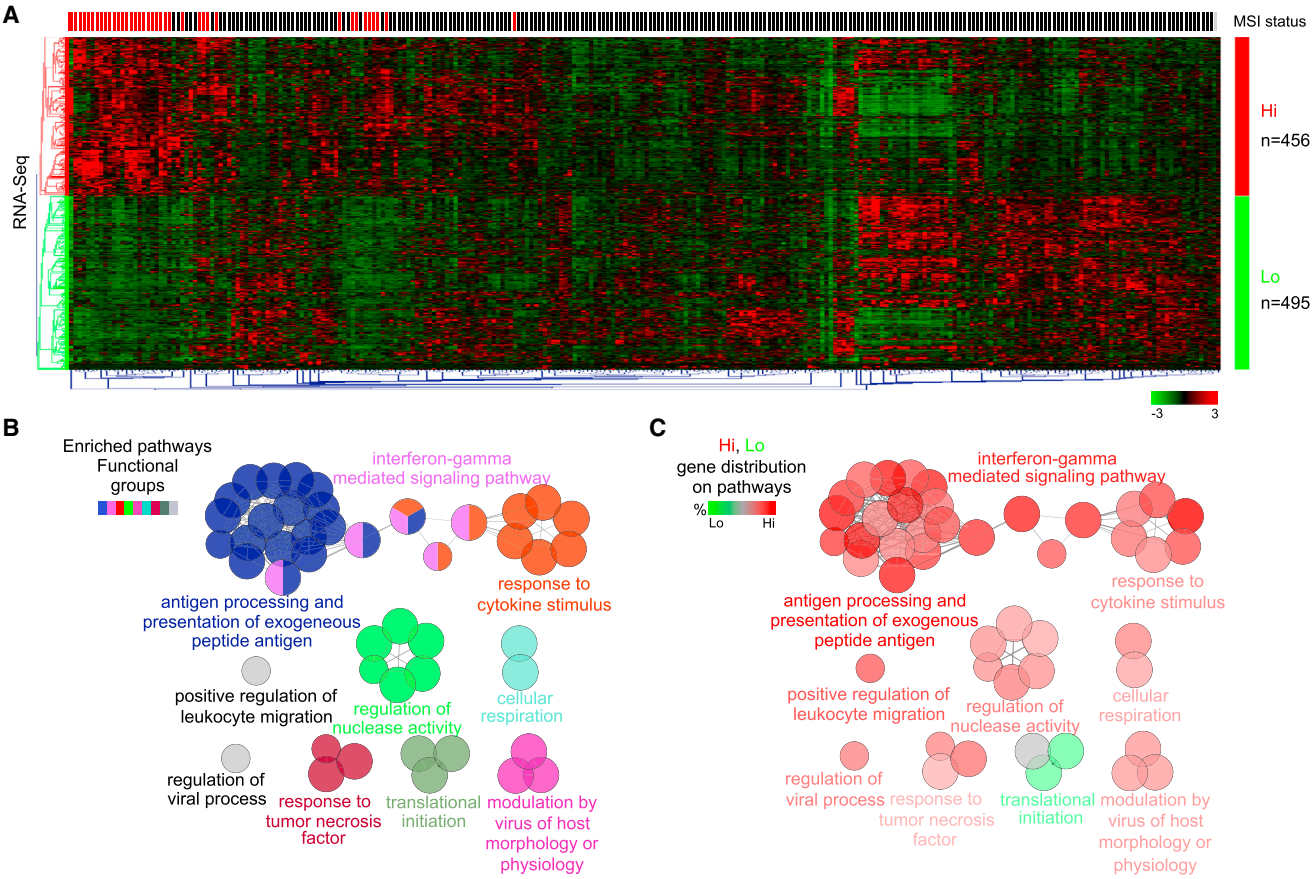

Figure 1. Integrative Analysis Reveals Overrepresented Pathways in MSI versus MSS Patients with CCR

(A) Integrative analysis of mRNA expression in cohort 1. MSI and MSS status is shown in red and black, respectively. 951 significantly differentially expressed genes ($p < 0.05$, Benjamini correction) in MSI versus MSS were investigated. Data were normalized and hierarchically clustered (Genesis, Euclidean distance, average linkage). High and low expression is shown by red and green, respectively. Two gene clusters, Hi (456 genes, red) and Lo (495 genes, green), were identified.

(B) Enriched functions and pathways of the 951 significantly differentially expressed genes in MSI versus MSS tumors. The network of pathways was created with the ClueGO and CluePedia Cytoscape apps. The pathways are functionally grouped and interconnected based on the kappa score. The size of the nodes shows the term significance after Bonferroni correction. The most significant term of each group is highlighted.

(C) The distribution of Hi and Lo gene clusters (A) on the pathway network (B). Pathways are colored in red and green based on the predominance of genes from Hi and Lo clusters, respectively. The color gradient shows the proportion of each gene cluster associated with the term. Equal proportion of the two clusters is shown in gray. See also Figure S1.

genes. All other immune population markers that were analyzed had similar expression in MSI and MSS tumors. Multiple cytokines and cytokine receptors had significantly increased expression in MSI tumors. In contrast, genes like *CCL24*, known to be upregulated in tumors (Tosolini et al., 2011), as well as *CXCL14*, *PRLR*, *ACVR1B*, and *TGFBR2*, which are potentially involved in epithelial to mesenchymal transition, were significantly more highly expressed in MSS tumors than in MSI tumors.

Transcript amounts of important soluble immune factors (*IFNG*, *IL15*, *GNLY*, *CCL3*, *CXCL16*) were increased, whereas *CXCL14* was decreased in patients with MSI (Figure 2B); these results were validated by qPCR in cohort 2 (Figure 2C). MSI patients in cohort 2 also had significantly increased expression of many immune-related genes (Figure S2A). However, a few MSI patients had a low expression of these genes in comparison to the rest of the MSI patients (Figure S2A). As in cohort 1, MSS patients were heterogeneous, with some patients exhibiting high expression of immune genes, similar to MSI patients. MSI patients had prolonged disease-free survival (DFS) times in comparison to MSS patients. Additionally, within the MSS group, the relapse risk differed depending on the immune gene expression. MSS patients with increased cytotoxic and Th1 gene expression had a significantly lower risk of relapse than MSS patients with low expression (Figure S2B) (HR [hazard ratio] = 2.1 [1.1–4.1], $p = 0.03$]). There was no significant difference in risk of relapse in patients with MSS and high immune expression (MSS-Hi), and those with MSI. In contrast, the patients with MSS and low immune expression (MSS-Lo) had a significantly higher risk of relapse than the MSI patients (HR = 3.2 [1.0–10.4], $p = 0.03$). In comparison to immune markers, half of the tumor-related genes were also highly expressed in MSI tumors; however, high expression of these genes in MSS patients did not impact the DFS (Figure S2C). Risk of relapse for MSS patients with either high or low expression of tumor-related genes was not

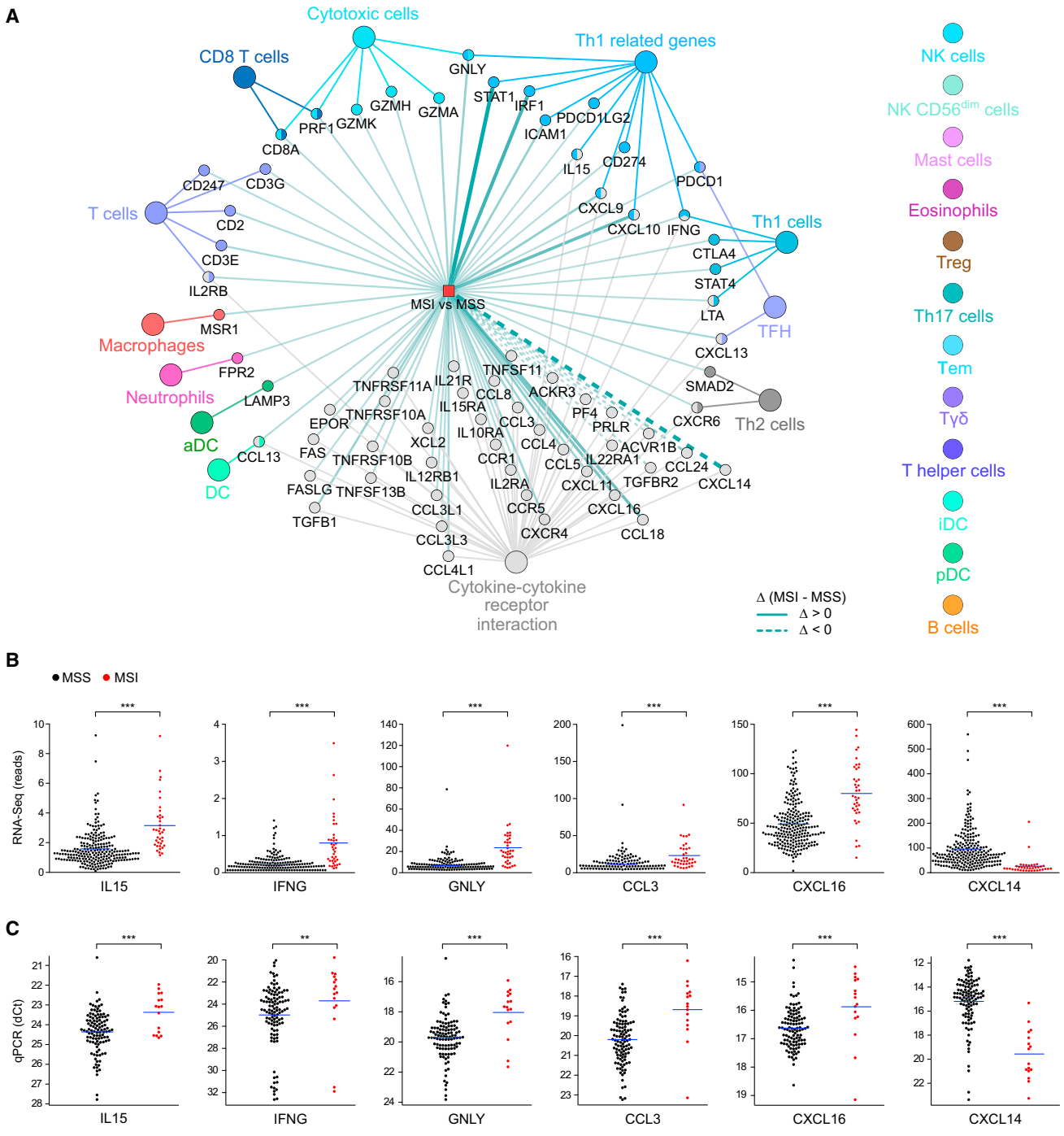

Figure 2. Immune Gene Expression in MSI and MSS CRC Patients

(A) Expression of immune cell markers (Immunome) was investigated in MSI and MSS patients (cohort 1) with the ClueGO and CluePedia Cytoscape apps. Markers with significantly different expression (Wilcoxon Mann-Whitney $p < 0.05$) are shown in a network. Markers associated to a cell type share the color of the node. The edges indicate the Δ difference of the log 2 expression values (MSI-MSS) of the respective node (gene). Negative Δ are shown with a discontinuous line.

(B) Gene expression in MSI (red) and MSS (black) patients from cohort 1 (RNA-seq).

(C) Gene expression in MSI (red) and MSS (black) patients from cohort 2 (qPCR low density array). Each dot represents an individual measurement of the gene expression in one individual. The mean values are indicated by blue dashes. Statistical analyses were performed by the unpaired t test method (***$p < 0.005$, **$0.005 >= p < 0.01$, *$0.01 >= p < 0.05$). See also Figure S2.

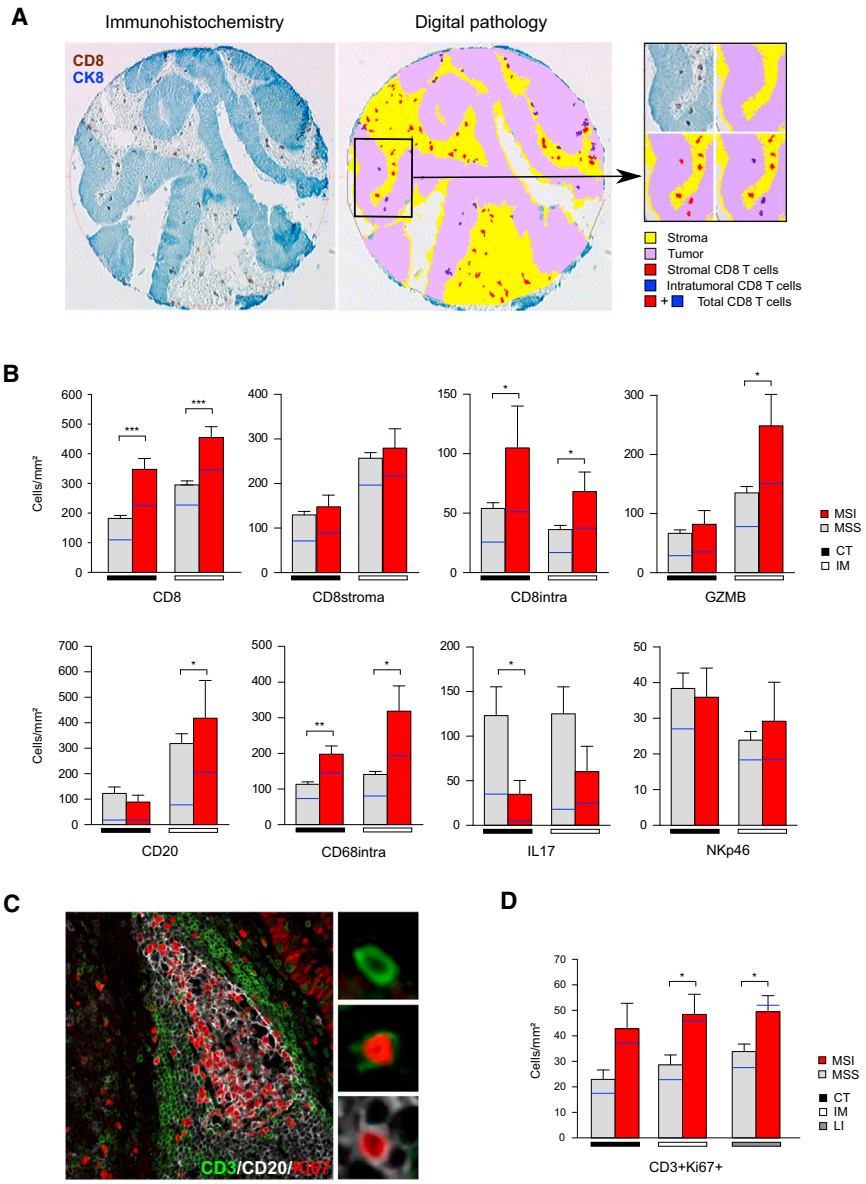

Figure 3. The Immune Cell Density in MSI and MSS CRC Patients

A) A representative example of CD8 immunostaining of a CRC tissue microarray (left) and the corresponding digital image (right). CD8 T cells (brown) and tumor cells (CK8, blue) are shown. The stroma is represented in yellow, the tumor in pink, and the stromal and intratumoral CD8 T cells are represented in red and blue, respectively. The immune cell densities were recorded as the number of positive cells per unit of tissue surface area. (B) Immune cell infiltrates in the CT (black) and in the IM (white) of tumors from MSI (red) and MSS (gray) patients (cohort 2). Tissue microarray measured immune density. Cytotoxic T (CD8 and GZMB), stromal cytotoxic T (CD8stroma), intratumoral cytotoxic T (CD8intra), B cells (CD20), macrophages (CD68 intra), Th17 (IL-17), and NK (NKp46) were quantified by immunohistochemistry. For CD8 and CD68, the cell densities were evaluated as total cell density, as stromal cells, and as intratumoral cells (within the tumor glands). The density of the cells was recorded as cells per mm^2. Bar charts represent the mean (± SEM) cell densities in the MSI and MSS patient groups, and the median cell count per mm^2 is in blue. The Wilcoxon Mann-Whitney method was applied (***$p < 0.005$, **$0.005 \geq p < 0.01$, *$0.01 \geq p < 0.05$). (C) T (CD3) and B (CD20) cell proliferation within CRC tumors. Cells positive for CD3, CD20, and Ki67 are shown in green, gray, and red, respectively. (D) Immune cell infiltrates in the CT (black) and in the IM (white) of tumors from MSI (red) and MSS (gray) patients (cohort 2). Bar charts represent the mean densities ± SEM of proliferating T cells (CD3+Ki67+) as cells per mm^2 of tissue in the CT, IM, and LIs. Statistical analyses were performed by the Wilcoxon Mann-Whitney method (***$p < 0.005$, **$0.005 \geq p < 0.01$, *$0.01 \geq p < 0.05$). See also Figure S2.

significantly different than that for MSI patients (HR = 2.9 [0.8–9.9], p = 0.06 and HR = 2.4 [0.7–7.7], p = 0.13).

Significant differences in mutational patterns and CIN were observed between MSI and MSS tumors. However, these genomic differences did not impact the survival of the patients. A prolonged survival was instead observed in MSI, as well as in a subgroup of MSS, tumors that had a prominent expression of Th1, cytotoxic genes, cytokines, and chemokines.

Increased Cytotoxic T cell, B cell, and Macrophage Densities in MSI Tumors

We next investigated the in situ immune response in the CT and IM of 490 CRC patients from cohort 2 by quantifying the number of cells (cells/mm^2) of the following type: $CD8^+$ T cells (Figure 3A), cytotoxic cells (detected with GZMB), B cells (CD20), macrophages (CD68), Th17 cells (interleukin 17 [IL-17]), and natural killer (NK) cells (NKp46). The total density of cytotoxic T cells was significantly higher in MSI samples than in MSS samples (Figure 3B). Because our previous research has shown that the precise intratumoral localization of infiltrating immune cells is very important (Bindea et al., 2013b; Galon et al., 2006), we measured $CD8^+$ T cell densities within the tumor glands (intratumoral) or within the stroma. MSI and MSS patients showed similar stromal $CD8^+$ T cell densities. However, there was a significant increase in the density of $CD8^+$ T cells within the tumor glands in MSI patients, in both the CT and IM (both $p < 0.05$). GZMB was also significantly increased in the IM of MSI patients ($p < 0.05$). The majority of the B cells accumulated at the IM and their density was significantly increased in MSI patients ($p < 0.05$). MSI patients also had a significantly higher mean CD68 density in the CT ($p < 0.001$), but not in the IM (Figure S2D). Furthermore, similar to the $CD8^+$ T cells, the macrophage infiltrate in the tumor glands was significantly higher in MSI in the CT ($p < 0.01$), as well as in the IM ($p < 0.05$). In contrast, the MSS patients showed a significantly increased Th17 infiltration in the CT ($p < 0.05$) and a very similar trend for the

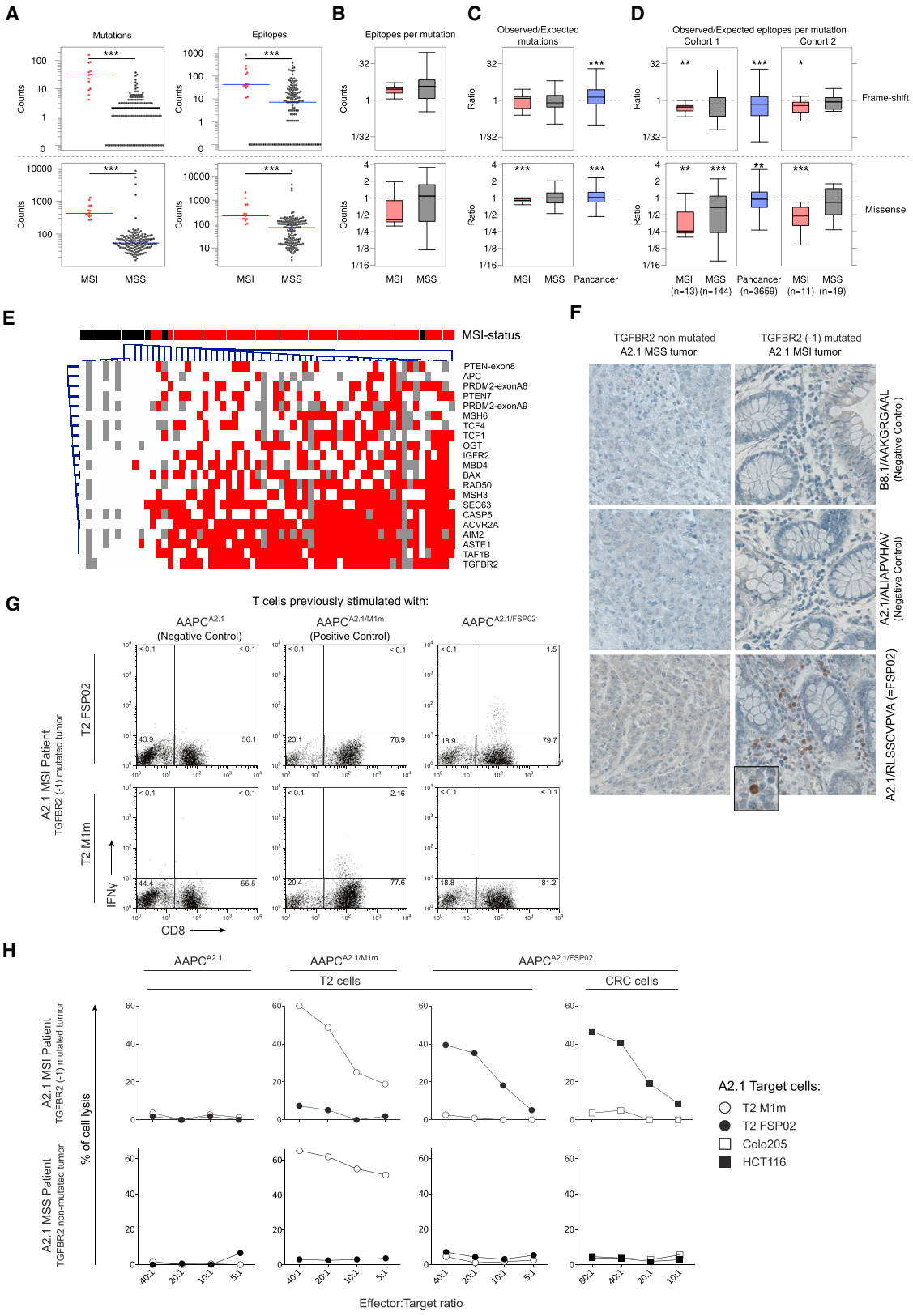

(legend on next page)

IM (Figure 3B). No differences in NK cell densities were observed. Together this demonstrates a significant increase in cytotoxic T cell, B cell, and macrophage infiltration in tumors from MSI patients.

High Frequency of Frameshift Mutations, Immunoediting, and Functional Specific Anti-tumor T Cells in MSI Tumors

One mechanism explaining enhanced immunogenicity of MSI tumors could be their increased cytokine expression (Figures 2A and 2B and S2A). For example, cytokines, such as IL-15, could influence the proliferation of locally infiltrating immune cells (Mlecnik et al., 2014). We quantified the density (cells/mm^2) of the in situ proliferating T (CD3$^+$Ki67$^+$) and B (CD20$^+$Ki67$^+$) cells within lymphoid islets (LIs), the IM, and the CT (Figure 3C). MSI patients had a significantly higher density of proliferating T cells than MSS patients did in the LIs ($p < 0.05$) and the IM ($p < 0.05$) and a higher total density in the CT (Figure 3D). The density of proliferating B cells was similar in MSI and MSS tumors (data not shown).

Another possibility is that, within the tumor microenvironment, genomic alterations (Figure S1B) of cytokines could modify their expression and affect in situ T cell proliferation. MSI patients had a significantly reduced frequency of CIN (Figure S1A).

In contrast, MSI tumors had a high mutational load followed by a significantly increased number of frameshift and missense mutations, as well as of neo-epitopes per tumor (Figure 4A). The increase in frameshift mutations appears to be an important resource of immunogenic mutations because the frequency of epitopes per frameshift mutation is higher than that per missense mutation. To determine whether the high mutational rate, and high immune infiltrate, observed in MSI tumors could result in immune editing, we tested whether the observed number of mutations or the number of epitopes per mutation was lower than expected (Figure 4B). The total number of frameshift and missense mutations was as expected for CRC and was independent of the microsatellite instability status. There was a significant drop in the number of neo-epitopes per mutation, but not in the number of mutations or silent mutations, in CRC, for both frameshift and missense mutations (Figures 4C and 4D). The deviation of the epitope rates from expectation was more pronounced in MSI tumors, with a 2-fold decrease in neo-epitopes for frameshift mutations and 4-fold decrease for missense mutations. These observations were confirmed in cohort 2 (Figure 4D).

Validation of these results with multiplex PCR showed that TGFBR2 frameshift mutations were very frequently detected in MSI, but not in MSS, tumors (Figure 4E).

For the majority of the analyzed genes, the mutations yielded neo-peptides with a high binding affinity to the most frequent HLA alleles (Figure S3A). Only three of the genes had no immunogenic mutations predicted to bind to HLA class I alleles. Many of the antigens were similar to TGFBR2, with mutations generating neo-epitopes predicted to bind to multiple HLA class I alleles. Several mutations also yielded neo-peptides for multiple HLA class II alleles (Figure S3B).

A tumor-specific T cell response toward the TGFBR2 (−1) mutation-derived neo-antigen was detected by immunohistochemistry with HLA-A*0201 molecules bearing a neo-epitope derived from this frameshift mutation (FSP02) in the primary tumor (Figure 4F and Figure S3C).

In order to demonstrate neo-antigen-specific T cell functionality in patients with CRC, we isolated peripheral TLs from six HLA-A*02 patients. Only the two MSI patients harboring the *TGFBR2* (−1) mutation in their tumor produced IFNγ (Figure 4G) and TNFα (Figure S3D) upon contact with T2 cells pulsed with FSP02 peptide and were able to specifically lyse T2 cells or a CRC cell line harboring the *TGFBR2* (−1) mutation (HCT116-HLA-A*0201 MSI) (Figure 4H).

These findings provide genetic evidence of immunoediting in human CRC and demonstrate that an effective anti-tumor immunity might naturally be elicited against true tumor-specific antigens resulting from somatic mutations.

Figure 4. Mechanisms Revealing a Higher Immunogenicity of MSI Patients

(A) The number of mutations and epitopes per tumor compared by microsatellite instability status, for two mutation types: frameshift (top row) and missense (second row). Microsatellite instability is indicated in red and microsatellite stability status in black. Wilcoxon rank-sum test was applied. ***$p < 0.001$.

(B–D) Box plots showing the interquartile range (IQR) of the number of epitopes per mutation (B), of the ratio observed versus expected number of mutations (C), and of the ratio observed versus expected epitopes per non-silent mutation (D). Median values are shown with a black line. The two hinges are versions of the first and third quartile. The whiskers extend 1.5 × IQR out of the box. MSI and MSS status are shown in red and gray, respectively.

(C) The average rate of frameshift and missense mutations per silent mutation was calculated across 3,659 tumors from 18 different cancer types (blue). Using this rate, the expected number of mutations was estimated from the number of silent mutations of the tumor, according to a previously published method.

(D) The number of epitopes per frameshift and missense mutation was estimated on the pan-cancer cohort (blue). Using this rate and the predicted number of frameshift and missense mutations, the expected number of epitopes per mutation is shown. The p values represent the deviation of the epitope rates from 1 when using the Wilcoxon rank-sum test. *$p < 0.5$, **$p < 0.01$, ***$p < 0.001$.

(E) Manually tested (20-plex) frameshift mutations in MSI and MSS patients (cohort 2). MSI and MSS are shown in red and black, respectively (color bar, top). Mutations are shown in red and their overrepresentation in MSI versus MSS patients is shown on the right. ***$p < 0.005$, **$0.005 \geq p < 0.01$, *$0.01 \geq p < 0.05$. No mutation is shown in white and missing data in gray.

(F) In situ immunohistochemistry toward HLA-A*0201/FSP02 complexes (FSP02: a TGFBR2 (−1) mutation-derived neoepitope).

(G and H) Activity of peripheral TLs from HLA-A*02+ patients (previously) stimulated on artificial antigen-presenting cells expressing no peptide of interest (AAPC$^{A2.1}$), M1m (AAPC$^{A2.1/M1m}$), or FSP02 peptide (AAPC$^{A2.1/FSP02}$).

(G) Flow cytometry analysis of activated TLs in contact with HLA-A*0201+ T2 cells pulsed with FSP02 (upper panels) or M1m (lower panel).

(H) Anti-tumor cytotoxic activity of activated TLs in contact with T2 cells pulsed with M1m or FSP02 peptide and with HLA-A*0201+ CRC-derived cell lines harboring (HCT116) or not (Colo205) the *TGFBR2* (−1) mutation. Higher panel shows cytotoxic activity profiles of TLs from a MSI patient harboring a *TGFBR2* (−1) mutant tumor. Profiles are representative of results obtained with two MSI patients with a *TGFBR2* (−1) mutant tumor. Lower panel shows cytotoxic activity profiles of TLs from a MSS patient. Profiles are representative of results obtained with four donors: two healthy individuals and two individuals with CRC who did not harbor the *TGFBR2* (−1) mutation in their tumor. See also Figure S3.

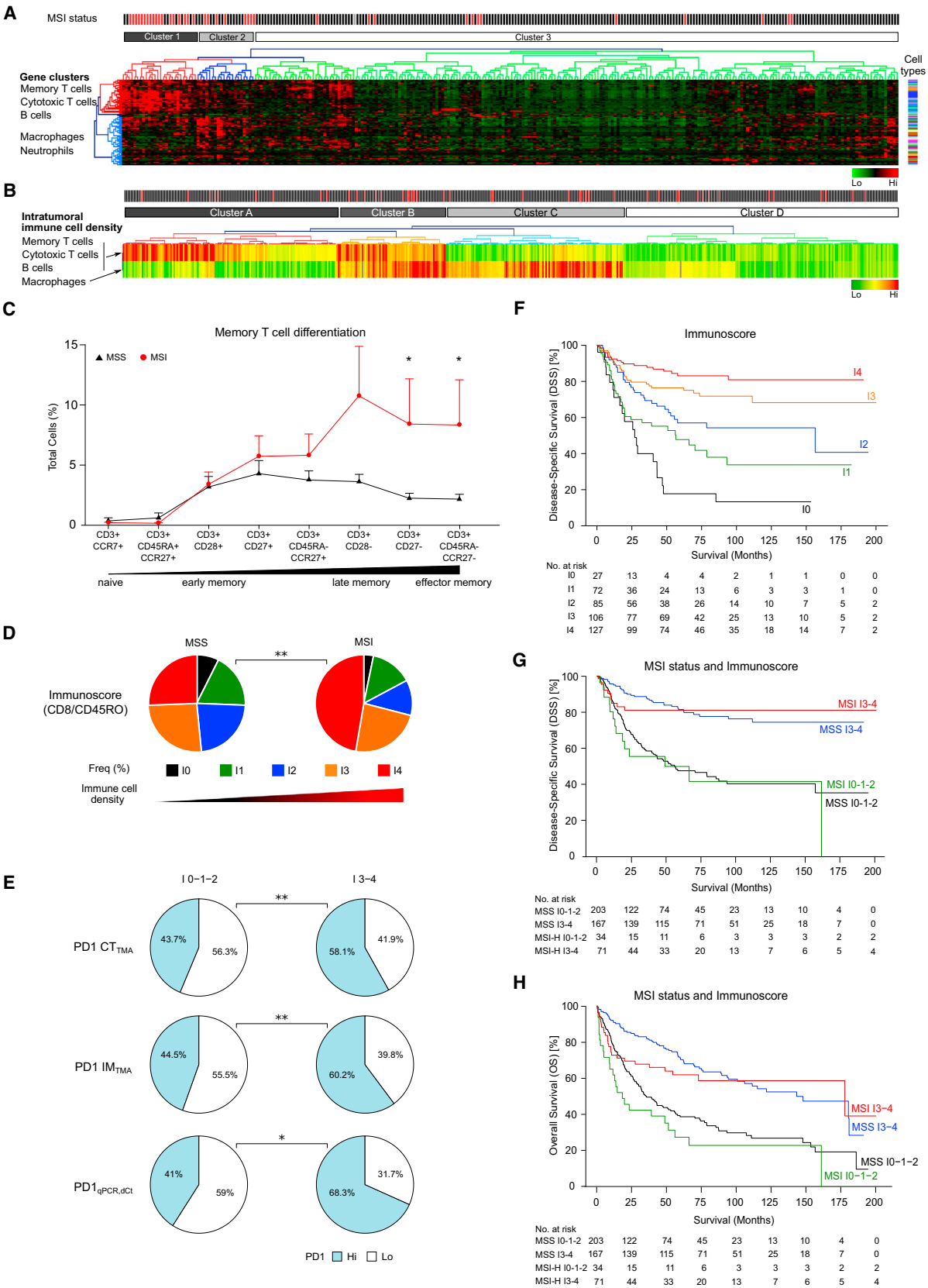

(legend on next page)

Immunoscore, but Not MSI and Tumor-Staging Parameters, Is Significant in Multivariate Analysis for DSS, DFS, and OS

Next, we further investigated the impact of microsatellite status and immune parameters on patient outcome (Figure 5). MSI and MSS patient groups were heterogeneous based on immunome (Bindea et al., 2013b) gene expression (Figure 5A). The MSI immune profiles included samples that either highly expressed T and B cell markers or macrophage and neutrophil markers (cluster 1, 2, 3). Some MSI patients had low expression of immune markers and were grouped with the MSS samples. We found similar findings by using immune cell densities to stratify patients (Figure 5B). One cluster of patients expressed higher density of both sets of markers. Patient clusters with high memory and cytotoxic T and B cells had prolonged disease-specific survival (DSS) (Figure S4A) regardless of the tumor's microsatellite instability status (Figure S4B). However, compared to T and B cells (Figure S4C), macrophage density did not influence DSS (Figure S4D). Interestingly, MSI patients did have increased infiltration of effector memory T cells ($CD3^+CD45RO^+CD45RA^-CCR7^-CD28^-CD27^-$) in comparison to MSS patients ($p < 0.05$) (Figure 5C).

Patients that had Immunoscore I4 tumors, highly infiltrated with $CD8^+$ and $CD45RO^+$ T cells in two locations of their tumor, were overrepresented in the MSI group in comparison to the MSS one ($p < 0.02$) (Figure 5D). We found similar results with Immunoscore when using CD3 and CD8 (data not shown). However, about 50% of MSS patients had a high Immunoscore (I3 or I4). Patients with a high Immunoscore had a significant overrepresentation of the frequency of cells expressing PD1 in the CT and IM, as well as increased expression of *PD1* mRNA (Figure 5E). Immunoscore I4 patients also had significantly better DSS (HR = 6.21 [3.42–11.27], p = 8.55E-12), DFS (HR = 6.35 [3.64–11.08], p = 6.8E-11), and overall survival (OS) (HR = 3.96 [2.42–6.47], p = 3.69E-9) (Figures 5F and S4E–S4I) than I0 patients who had very low densities of T cells in the CT or IM. Survival analysis of groups, defined based on both microsatellite status and Immunoscore, showed that patients with high cytotoxic and memory immune infiltrate (I3 and I4) had prolonged DSS (Figure 5G and S4J), OS (Figure 5H, S4K), and DFS (Figures S4L and S4M) despite their microsatellite status. MSI and MSS patients with a low Immunoscore (I0–I2) had a higher risk of relapse (Figure S4M), shorter DSS (HR = 2.4 [1.1–5.24], p = 0.023 and HR = 3.4 [2.3–5.05], p = 6.9E-11, respectively), and shorter OS (HR = 1.8[1.04-3.11], p = 0.033 and HR = 2.43[1.81-3.26], p = 1E-9, respectively) than patients with a high Immunoscore (I3 or I4) (Figures 5G, 5H, and S4K–S4M).

The heterogeneity of the immune infiltrate observed within MSI and MSS tumors could have multiple causes. Immune densities (Figures S5A–S5C) and the frequency of high Immunoscores (I3 or I4) were significantly higher in patients with Lynch syndrome than in the MSS patients (Figures S5D and S5E) (Popat et al., 2005), but no significant difference was observed between MSI patients and patients with Lynch syndrome (Figures S5F and S5G). The source of microsatellite instability was not a determinant of the tumor infiltrate.

WNT/β-catenin pathway mutations occur in the majority (70%) of the MSS patients (Figures S1A and S5H) and could potentially influence the immune infiltrate, as recently described in melanoma (Spranger et al., 2015). However, these mutations had no impact on the expression of Th1 or cytotoxic gene expression in MSS tumors (Figures S5I and S5J). The CD3 and CD8 infiltrate was not significantly different in patients with or without WNT/β catenin pathway mutations (Figures S5K and S5L). A subgroup of MSI tumors with WNT/β-catenin mutations showed a strong increase in *GNLY* and *GZMA* expression in comparison to the rest of the MSI patients (Figure S5I), whereas intratumoral CD8 and PD1 infiltrates were decreased in the CT (Figure S5L). The frequency of high and low Immunoscore patients with WNT/β-catenin mutations was similar (Figure S5M). WNT/β-catenin pathway mutations did not significantly influence the immune gene expression and infiltrate within MSI or MSS patients.

The amounts of intratumoral PD1 and PDL1 could also influence the response to therapies. In agreement with previous reports (Llosa et al., 2015), significantly different amounts of PD1 *(PDCD1)* and PDL1 *(CD274)* were observed in MSI and MSS

Figure 5. Immunoscore As a Survival Predictor among Stage I–IV CRC Patients

(A) The expression of 81 immune subpopulation markers in patients with CRC (cohort 1). MSI patients are shown in red and MSS patients in black. RNA-seq data were normalized and hierarchically clustered. High and low expression is represented in red and green, respectively. The MSI patient cluster with high T (*CD4*, *CD8*, *GZMB*, *CD45RO*) and B (*CD20*) cell (red gene cluster) gene expression is shown in dark gray. The MSI patient cluster with high expression of macrophage and neutrophil genes (blue gene cluster) is shown in light gray. The MSS cluster is shown in white.

(B) Immune cell infiltrates in CRC patients (cohort 2) measured by immunohistochemistry analysis of tissue microarrays.Mean density of CD8, CD45RO, GZMB, CD20, and CD68 was calculated for each patient. Data were normalized and hierarchically clustered in Genesis (Pearson uncentered, complete linkage). High and low densities are shown in red and green, respectively. Patient clusters A and B with high density of memory and cytotoxic T cells and B cells are marked in dark gray. The high macrophage cluster C is shown in light gray. The low immune density cluster D is white.

(C) Memory T cell differentiation in MSI (red circle) and MSS (black triangle) patients. Four-color flow-cytometric analysis of T cell populations present in freshly resected CRC tumors according to the percentage of CD3+CD5+ cells and the microsatellite instability status. Immune cell populations were represented as the mean percentage (± SEM) of positive cells for specific marker combinations. The Mann-Whitney test was applied (*$p < 0.05$).

(D) The frequency of Immunoscore-based groups (I0, I1, I2, I3, I4) in MSS and MSI patients. Immunoscore summarizes the density of memory (CD45RO) and cytotoxic (CD8) T cells in the CT and in the IM of the tumor. Five groups of patients were defined based on the high (Hi) density of those two markers in the CT and IM. Minimum p value cutoff: I0 (0 Hi, black), I1 (1 Hi, green), I2 (2 Hi, blue), I3 (3 Hi, orange), I4 (4 Hi, red).

(E) Frequency of the 50% highest PD1 (Hi, blue) and 50% lowest (Lo, white) patients in Immunoscore categories I0–I2 and I3 and I4. PD1 density was measured as cells per mm^2 by tissue microarrays in the CT and the IM of the tumor. *PD1* mRNA expression was measured by qPCR dCt.

(F) Kaplan-Meier estimates of disease-specific survival according to Immunoscore.

(G) Kaplan-Meier estimates of disease-specific survival according to the microsatellite instability status and Immunoscore. Patients with scores I0, I1, and I2 were pooled. Patients with scores I3 and I4 were pooled.

(H) Kaplan-Meier estimates of overall survival according to the microsatellite instability status and Immunoscore. Patients with scores I0, I1, and I2 were pooled. Patients with scores I3 and I4 were pooled. See also Figures S5 and S6.

Table 1. Multivariate Cox Proportional Hazard Model for DSS among Cohort 2 Patients with AJCC and UICC TNM Stage I–III CRC

Variable	PHA Test[a]	HR (95% CI)	p Value
DSS, Model 1			
MSI status	0.0872	1.33 (0.69–2.57)	0.3951
Immunoscore	0.2918	0.6 (0.5–0.73)	0.0001[b]
DSS, Model 2			
MSI stage	0.1325	1.27 (0.65–2.45)	0.4870
AJCC and UICC TNM stage	0.0180‡	1.27 (0.87–1.85)	0.2127
Immunoscore	0.1331	0.62 (0.51–0.75)	0.0001[b]
Before Stepwise (stepAIC) Selection			
MSI status	0.5811	0.92 (0.45–1.9)	0.8280
Sex	0.5774	1.31 (0.78–2.19)	0.3047
Tumor (T) stage	0.0918	1.23 (0.83–1.81)	0.3026
N stage	0.4403	1.32 (0.77–2.27)	0.3158
Histologic grade	0.4943	1.08 (0.65–1.78)	0.7789
VELIPI	0.1206	0.52 (0.3–0.92)	0.0235[b]
Mucinous colloid type	0.7579	1.03 (0.57–1.88)	0.9205
Occlusion	0.9315	0.7 (0.3–1.65)	0.4187
Perforation	0.2791	2.48 (0.81–7.65)	0.1124
Immunoscore	0.0770	0.63 (0.51–0.77)	0.0001[b]
Final Model after Stepwise (stepAIC) Selection			
MSI status	0.3951	1.02 (0.51–2.05)	0.9496
VELIPI	0.0253	0.45 (0.27–0.76)	0.0029[b]
Perforation	0.2129	2.68 (0.92–7.81)	0.0704
Immunoscore	0.1347	0.61 (0.5–0.74)	0.0001[b]

The final model was built based on 367 patients. All categorical covariates were transformed into numeric codes before they were added to the Cox model. Numeric codes are as follows. AJCC and UICC TNM stage: stage I = 0, stage II = 1, stage III = 2. Immunoscore (CD8 and CD45RO were quantified in the center and invasive margin of the tumor, minimum p value cutoff with four groups): I0 = 0 (0 Hi), I1 = 1, I2 = 2, I3 = 3, I4 = 4 (4 Hi). T stage (histopathologic criteria of tumor invasion): Tis (in situ) and T1 = 0, T2 = 1, T3 = 2, T4 = 3. N stage (spread to local lymph nodes): N0 = 0, N+ = 1. Sex: male = 0, female = 1. Histological grade: well differentiated = 0, moderately differentiated = 1, poorly differentiated = 2. VELIPI, mucinous colloid type, occlusion, bowel perforation: no = 0, yes = 1. MSI status: MSS = 0, MSI = 1. Abbreviations are as follows: DSS, disease-specific survival; AJCC and UICC TNM, the American Joint Committee on Cancer and the International Union Against Cancer TNM staging system; VELIPI, vascular emboli, lymphatic invasion, and perineural invasion; PHA, proportional hazards assumption; HR, hazard ratio; AIC, Akaike information criterion; MSI, microsatellite instability. The new Bethesda panel was used (Bacher et al., 2004).

[a]PHA test p < .05 violates the hazards assumption. If a marker in the final model violates the hazards assumption, the model will be adjusted for this marker.

[b]Significant.

patients from cohort 1 (Figure S6A), as well as in immunome-defined clusters (Figures S6B and S6C). The highest *PDCD1* and *CD274* expression was measured in MSI patients from cluster 1, which is characterized by high expression of genes associated with memory and cytotoxic T cells, as well as B cell markers (Figures S5I and S5J). Confirming these results, high Immunoscore (I3 and I4) patients from cohort 2 had significantly higher *PDCD1* and *CD274* expression than I0–I2 patients did (Figure S6D), independent of their microsatellite status (Figure S6E). Significantly increased *PDCD1* expression was also observed in I3 and I4 MSS patients, in comparison to that in I 0-1-2 MSS patients. Tissue microarray analyses performed in cohort 2 revealed that the density of PD-1 expressing cells in the two Immunoscore groups (I0–I2 and I3 and I4) was significantly different in MSI patients than in MSS patients (Figure S6F). PD1 density was increased in I3 and I4 patients (Figure S6G), independent of their microsatellite status (Figure S6H). Such patients might potentially benefit from an anti-PD1 therapy. All experiments are summarized in Figure S6I.

In a Cox multivariate regression model combining Immunoscore with T-stage, N-stage, sex, VELIPI, histological grade, mucinous-colloide type, occlusion, perforation, and the microsatellite status, only Immunoscore and VELIPI remained significant and were kept after stepwise Akaike-information-criterion (AIC)-based Cox multivariate analysis for DSS (Table 1). For DFS and OS, the microsatellite instability status, T stage, and N stage were no longer significant, whereas Immunoscore remained significant (p = 0.0001) for determining patient outcome (Table S2). VELIPI was only significant for DSS and DFS, whereas the perforation was only significant for OS. Thus, Immunoscore remained significant in multivariate analysis for DSS, DFS and OS, whereas the histopathological parameters and microsatellite instability status did not.

DISCUSSION

Here, we performed a comprehensive analysis of tumor cell features and tumor microenvironment and immune parameters in three cohorts of patients (INSERM cohort 2, n=689; TCGA CRC cohort 1, n=270; TCGA pan-cancer cohort 3, n=3,659) in relation with the microsatellite instability status. Tumors can be classified on the basis of multiple morphologic, phenotypic, and functional factors, including the presence of microsatellite instability (Galon et al., 2014). It has been reported that some, but not all, published studies found an independent prognostic value of the microsatellite instability status for survival (Popat et al., 2005).

The mechanism by which the presence of a high frequency of frameshift mutations in microsatellite instability might influence clinical outcome is still unknown. One hypothesis could be related to the kinds of mutations that occur following the damage of the DNA MMR system. We found that MSI tumors had fewer mutations of *APC*, *KRAS*, and *TP53* and more frequent mutations in *ACVR2A*, *FBXW7*, and the β-catenin (*CTNNB1*) genes than MSS tumors did, as previously reported (Westra et al., 2004). We also confirmed that MSI tumors had less CIN than MSS tumors did. However, none of these mutations, nor the CIN score, were associated with a significant difference in survival and therefore might not have a direct contribution to the positive prognostic value of microsatellite instability. In comparison, mutational load was associated with the degree of clinical benefit in melanoma (Snyder et al., 2014) and with durable clinical benefit to anti-PD1 and progression-free survival in lung cancer (Gubin et al., 2014).

An alternative hypothesis relates to the effect of microsatellite instability on an anti-tumor immune response (Angelova et al.,

2015). Our data demonstrate that a high frequency of frameshift mutations in microsatellite instability might influence clinical outcome by increasing the presence and functionality of tumor-specific effector memory T cells. MSI patients and patients with Lynch syndrome have a similar intratumoral immune density (Tougeron et al., 2013). Several large CRC studies have demonstrated that semi-quantification of T cell subpopulations is significantly associated with good prognosis, even after adjusting for stage, lymph node count, and molecular biomarkers, including microsatellite instability (Nosho et al., 2010; Ogino et al., 2009). Furthermore, the prognostic value associated with $CD3^+$, $CD8^+$, and $CD45RO^+$ T cell infiltration in CRC has been demonstrated (Zlobec et al., 2010).

The importance of tumor-specific mutant antigens as targets of checkpoint blockade therapy, as well as for personalized cancer-specific vaccines, has been demonstrated in mouse models (Gubin et al., 2014). In humans, evidence for immunoediting has been reported (Rooney et al., 2015), but the experimental challenges of monitoring the in vivo expansion of potential anti-tumor effector T cells, to assess both the quality and amplitude of an anti-tumor response, mean that there is limited data regarding in situ responses to specific antigenic epitopes. Here, using genetic evidence (exome sequencing data) and immunogenic peptide predictions, we demonstrated that immunoediting of immunogenic frameshift and missense mutations occurs in CRC, and that it occurs more frequently in MSI tumors. Such an immunogenic epitope suitable for mutation-specific vaccination was recently described in glioma (Schumacher et al., 2014; Schumacher and Schreiber, 2015).

We showed that a tumor-specific T cell response toward a mutated TGFBR2 class I neo-epitope could be detected in the primary tumor. Additionally, peripheral cytotoxic T cells from MSI patients specifically killed an HLA-matched MSI tumor cell line (in vitro). The cytotoxic activity was not restricted to one particular epitope, given that other peptides derived from frameshift mutations (ASTE1 and TAF1B) could be targeted by cytotoxic T cells of HLA-A*0201 MSI patients (data not shown). Our study demonstrates that strong and effective anti-tumor immunity might naturally be elicited against true tumor-specific antigens resulting from somatic mutations. Given that frameshift mutations are more common in MSI patients, mainly because of epigenetic silencing of a MMR gene, MSI patients might be expected to generate more targetable neoantigens. The anti-tumor immunity phenotype might be shaped by a combination of multiple tumor parameters, including microsatellite instability, altered HLA expression, expression of tumor antigens, the mutational pathways (CpG-island methylator phenotype, or chromosome instability), and microenvironmental factors (Angell and Galon, 2013; Finn, 2006; Fridman et al., 2012; Ogino et al., 2011). Here, we showed that among MSI patients, only the ones with Immunoscores I3 and I4 have prolonged DSS.

The immune infiltrate heterogeneity observed in MSI tumors could be related to WNT/β-catenin pathway mutations, as recently described in melanoma (Spranger et al., 2015). MSI patients with a mutation had a decreased intratumoral CD8 density and a reduced $PD1^+$ infiltrate in the CT in comparison to the other MSI patients, thus their response to immune checkpoint therapies could be impaired. Moreover, among MSS patients, the ones with a high Immunoscore (I3 or I4) have a prolonged DSS, as well as increased *PDCD1* expression and density in comparison to that of low Immunoscore MSS patients. Cox multivariate analysis, combining the histopathological features of the tumor (including T-stage and N-stage), microsatellite instability status, and Immunoscore, supports the advantage of Immunoscore over microsatellite instability in predicting recurrence and survival. We demonstrated a statistical dependence between the microsatellite instability and the immune criteria, with a superiority of the Immunoscore, given that it also predicts outcome in MSS patients. Thus, it can be hypothesized that at least part of the prognostic value of the microsatellite instability status could be attributed to major underlying differences of quality and density of infiltrating immune cells. It was also shown that MSI tumors contain a higher frequency of frameshift mutations, which can lead to immunogenic peptides, as demonstrated by the existence of anti-frameshift mutation peptide-specific T cells within the tumor.

Immune parameters associated with microsatellite instability could also have an impact on patient response to therapeutics. It was initially shown that fluorouracil-based adjuvant chemotherapy benefited stage II or III MSS patients, but not those with MSI tumors (Ribic et al., 2003), although this is not confirmed in all studies (Des Guetz et al., 2009). Chemotherapeutic agents can stimulate immunogenic cell death (Vacchelli et al., 2012) and can mediate therapeutic effects by reactivating pre-existing tumor-specific immune responses (Fridman et al., 2012; Galon et al., 2013). Frequent frameshift mutations from MSI patients could also provide potential targets for cancer vaccines. Vaccine approaches encompassing commonly mutated peptides could be particularly well-suited for MSI patients, given that these peptides might provide a boost to a potentially pre-existing immune response.

Similarly, recent advances in cellular immunology and tumor biology are guiding new approaches to adoptive T cell therapy (June, 2007) that have been reported to mediate potent tumor regression in metastatic cancers (Grupp et al., 2013; Restifo et al., 2012). As MSI patients present generally enhanced cytotoxic T cell responses, these naturally infiltrating T cells (Bindea et al., 2013b) provide efficient immunotherapy approaches to treat cancer, as recently illustrated in clinical trials boosting T cells responses with anti-CTLA4 (Hodi et al., 2010; Robert et al., 2011), anti-PDCD1 (PD-1) (Des Guetz et al., 2009; Topalian et al., 2012), and anti-CD274 (PD-L1) (Brahmer et al., 2012). There are clinical trials in MSI metastatic patients supporting the efficacy of anti-PD1 (Le et al., 2015). Our data would argue (1) that MSI patients at an early stage might benefit the most from checkpoint T cell therapies, given that they have a strong effector T cell response and more frequently present a high Immunoscore associated with augmented PD1 expression, (2) that only a subgroup of metastatic MSI patients might benefit from checkpoint T cell therapies, namely those having a high Immunoscore, and (3) that MSS patients with tumors highly infiltrated with immune cells could also benefit from the therapy.

Thus, the immune infiltration and Immunoscore should better define the prognosis of CRC patients, better identify patients at high risk of tumor recurrence regardless of MSI, and help to

predict and stratify patients who will benefit from immunotherapies (Church and Galon, 2015; Galon et al., 2013).

EXPERIMENTAL PROCEDURES

Patients with CRC were analyzed from two different cohorts. For cohort 1, we analyzed 270 CRC patients from the TCGA dataset (Cancer Genome Atlas, 2012). For cohort 2, analysis was done on 694 tissue samples collected at the Laennec-HEGP Hospitals (Paris) and Rouen Hospital (Rouen) from CRC patients who underwent primary resection of their tumor. Histopathological and clinical findings were scored according to the UICC TNM staging system (Table S1). Microsatellite instability status was assessed with the classical molecular new Bethesda panel (with markers BAT25, BAT26, NR21, NR24, and NR27). High MSI (MSI-H) patients were characterized and compared to the rest of the cohort, low MSI (MSI-L) and MSS patients. In addition, D2S123, D17S250, D5S346, BAT40, MYCL, and NR22 microsatellites were tested on 606 patients from cohort 2. Multiple techniques were used to investigate the tumor microenvironment, including quantitative real-time TaqMan PCR expression profiling with low-density arrays (Applied Biosystems). Immunohistochemistry on tissue microarray sections was performed to characterize and quantify the tumor immune infiltrate. Specifically, we quantified Immunoscore by using CD3 and CD8 or CD8 and CD45RO staining in the CT and IM. Immunoscore I4 is when two markers (CD3, CD8, or CD45) have high density in both tumor regions (CT and IM). Immunoscore I0 is when a patient has low density for two markers in both tumor regions, and Immunosocores I1–I3 represent intermediate scores (Galon et al., 2014). Fluorescent immunohistochemistry was performed to evaluate the presence of proliferating B ($CD20^{+}Ki67^{+}$) and T ($CD3^{+}Ki67^{+}$) cells. Digital quantification of cell densities was performed (Definiens). Intratumoral cells from fresh tumors were analyzed by flow cytometry (FACS) with a FACScalibur flow cytometer (Becton Dickinson). Intratumoral antigen-specific T cells were detected with immunohistochemistry with HLA-A*0201+ dextramer (Immudex). Genomic alterations were estimated via array comparative genomic hybridization and the whole-genome oligonucleotide microarray platform (44B, Agilent Technologies). Whole-exome sequencing was performed on an Illumina HiSeq 2000 for 30 CRC patients (IntegraGen). A QIAamp DNA FFPE Tissue Kit (QIAGEN) and fluorescent multiplex PCR assays (Applied Biosystems) were used to detect frameshift mutations. HLA-A*0201 artificial antigen-presenting cells were constructed, and cytotoxicity assays with antigen-specific T lymphocytes were performed with standard ^{51}Cr release assays. In brief, peripheral T lymphocytes (TLs) of six HLA-A*02 CRC patients were stimulated two times on artificial antigen-presenting cells, $AAPC^{A2.1/FSP02}$. TLs were then analyzed for intracellular cytokine expression and lytic ability in response to T2 lymphoblast cells pulsed with FSP02 or an HLA-A*0201 MSI CRC-derived cell line (HCT116) harboring a *TGFBR2* (−1) mutation, that is, a deletion of one adenine in a 10-adenine-repeat sequence.

Tumor microenvironment data were analyzed with ClueGO (Bindea et al., 2009) and CluePedia (Bindea et al., 2013a), apps of Cytoscape (Shannon et al., 2003), and with the software R implemented as a statistical module in TME.db. All p values were two sided. A p value <0.05 was considered statistically significant. Ethical, legal, and social implications were approved by institutional ethical review boards. All experiments were performed according to the Helsinki guidelines. Details regarding materials and methods are provided in the Supplemental Experimental Procedures.

SUPPLEMENTAL INFORMATION

Supplemental Information includes Supplemental Experimental Procedures, six figures, and two tables and can be found with this article online at http://dx.doi.org/10.1016/j.immuni.2016.02.025.

AUTHOR CONTRIBUTIONS

H.K.A., P.M., S.E.C., L.L., M.F., T.F., M.S., A.M.B., A.K., A.C.O., and M.H. acquired the tumor microenvironment data. P.M., M.A., and A.R. acquired the genomic data. B.M., G.B., M.A., H.K.A., and P.M. analyzed the data. A.B. was responsible for clinical data. M.H., A.B., P.B., J.J.T., J.C.S., F.L.P., J.M., A.R., P.L.P., P.M., R.S., T.F., and F.P. were responsible for sample collection and access to patients. B.M., G.B., F.P., V.V.A., J.B.L., and J.G. interpreted the microenvironment data. B.M. G.B., M.A., M.R.S., Z.T., J.B.L., and J.G. interpreted the genomic data. J.G. designed and supervised the study. B.M., G.B., J.B.L., and J.G. wrote the manuscript. B.M., G.B., H.K.A., P.M., M.A., F.P., V.V.A., J.B.L., and J.G. revised the manuscript.

ACKNOWLEDGMENTS

This work was supported by grants from the National Cancer Institute of France (INCa), the Canceropole Ile de France, MedImmune, INSERM, the Austrian Federal Ministry of Science and Research (GEN-AU project Bioinformatics Integration Network), the Qatar National Research Fund under its National Priorities Research Program award number NPRP09-1174-3-291, the European Commission (7FP, Geninca Consortium, grant 202230), the Transcan ERAnet European project, the Association pour la Recherche contre le Cancer (ARC), the Advanced Bioinformatics Platform for Personalised Cancer Immunotherapy (APERIM), Horizon 2020 (PHC-32 grant 633592), INSERM and the Haute-Normandie Region (who provided a PhD fellowship for P.M.), La Ligue Contre le Cancer de Haute-Normandie, the Cancer Research For Personalized Medicine (CARPEM), the Paris Alliance of Cancer Research Institutes (PACRI), and the LabEx Immuno-oncology.

Received: June 5, 2015
Revised: October 12, 2015
Accepted: November 25, 2015
Published: March 15, 2016

REFERENCES

Angell, H., and Galon, J. (2013). From the immune contexture to the Immunoscore: the role of prognostic and predictive immune markers in cancer. Curr. Opin. Immunol. *25*, 261–267.

Angelova, M., Charoentong, P., Hackl, H., Fischer, M.L., Snajder, R., Krogsdam, A.M., Waldner, M.J., Bindea, G., Mlecnik, B., Galon, J., and Trajanoski, Z. (2015). Characterization of the immunophenotypes and antigenomes of colorectal cancers reveals distinct tumor escape mechanisms and novel targets for immunotherapy. Genome Biol. *16*, 64.

Atreya, I., and Neurath, M.F. (2008). Immune cells in colorectal cancer: prognostic relevance and therapeutic strategies. Expert Rev. Anticancer Ther. *8*, 561–572.

Bacher, J.W., Flanagan, L.A., Smalley, R.L., Nassif, N.A., Burgart, L.J., Halberg, R.B., Megid, W.M., and Thibodeau, S.N. (2004). Development of a fluorescent multiplex assay for detection of MSI-High tumors. Dis. Markers *20*, 237–250.

Berghoff, A.S., Fuchs, E., Ricken, G., Mlecnik, B., Bindea, G., Spanberger, T., Hackl, M., Widhalm, G., Dieckmann, K.D., Bilocq, A.M., et al. (2016). Density of tumor-infiltrating lymphocytes correlates with extent of brain edema and overall survival time in patients with brain metastases. OncoImmunology *5*, e1.

Bindea, G., Mlecnik, B., Hackl, H., Charoentong, P., Tosolini, M., Kirilovsky, A., Fridman, W.H., Pagès, F., Trajanoski, Z., and Galon, J. (2009). ClueGO: a Cytoscape plug-in to decipher functionally grouped gene ontology and pathway annotation networks. Bioinformatics *25*, 1091–1093.

Bindea, G., Galon, J., and Mlecnik, B. (2013a). CluePedia Cytoscape plugin: pathway insights using integrated experimental and in silico data. Bioinformatics *29*, 661–663.

Bindea, G., Mlecnik, B., Tosolini, M., Kirilovsky, A., Waldner, M., Obenauf, A.C., Angell, H., Fredriksen, T., Lafontaine, L., Berger, A., et al. (2013b). Spatiotemporal dynamics of intratumoral immune cells reveal the immune landscape in human cancer. Immunity *39*, 782–795.

Bindea, G., Mlecnik, B., Angell, H.K., and Galon, J. (2014). The immune landscape of human tumors: Implications for cancer immunotherapy. OncoImmunology *3*, e27456.

Brahmer, J.R., Tykodi, S.S., Chow, L.Q., Hwu, W.J., Topalian, S.L., Hwu, P., Drake, C.G., Camacho, L.H., Kauh, J., Odunsi, K., et al. (2012). Safety and

activity of anti-PD-L1 antibody in patients with advanced cancer. N. Engl. J. Med. *366*, 2455–2465.

Broussard, E.K., and Disis, M.L. (2011). TNM staging in colorectal cancer: T is for T cell and M is for memory. J. Clin. Oncol. *29*, 601–603.

Cancer Genome Atlas Network (2012). Comprehensive molecular characterization of human colon and rectal cancer. Nature *487*, 330–337.

Church, S.E., and Galon, J. (2015). Tumor Microenvironment and Immunotherapy: The Whole Picture Is Better Than a Glimpse. Immunity *43*, 631–633.

Des Guetz, G., Schischmanoff, O., Nicolas, P., Perret, G.Y., Morere, J.F., and Uzzan, B. (2009). Does microsatellite instability predict the efficacy of adjuvant chemotherapy in colorectal cancer? A systematic review with meta-analysis. Eur. J. Cancer *45*, 1890–1896.

Finn, O.J. (2006). Human tumor antigens, immunosurveillance, and cancer vaccines. Immunol. Res. *36*, 73–82.

Finn, O.J. (2008). Cancer immunology. N. Engl. J. Med. *358*, 2704–2715.

Fridman, W.H., Pagès, F., Sautès-Fridman, C., and Galon, J. (2012). The immune contexture in human tumours: impact on clinical outcome. Nat. Rev. Cancer *12*, 298–306.

Galon, J., Costes, A., Sanchez-Cabo, F., Kirilovsky, A., Mlecnik, B., Lagorce-Pagès, C., Tosolini, M., Camus, M., Berger, A., Wind, P., et al. (2006). Type, density, and location of immune cells within human colorectal tumors predict clinical outcome. Science *313*, 1960–1964.

Galon, J., Pagès, F., Marincola, F.M., Angell, H.K., Thurin, M., Lugli, A., Zlobec, I., Berger, A., Bifulco, C., Botti, G., et al. (2012a). Cancer classification using the Immunoscore: a worldwide task force. J. Transl. Med. *10*, 205.

Galon, J., Pagès, F., Marincola, F.M., Thurin, M., Trinchieri, G., Fox, B.A., Gajewski, T.F., and Ascierto, P.A. (2012b). The immune score as a new possible approach for the classification of cancer. J. Transl. Med. *10*, 1.

Galon, J., Angell, H.K., Bedognetti, D., and Marincola, F.M. (2013). The continuum of cancer immunosurveillance: prognostic, predictive, and mechanistic signatures. Immunity *39*, 11–26.

Galon, J., Mlecnik, B., Bindea, G., Angell, H.K., Berger, A., Lagorce, C., Lugli, A., Zlobec, I., Hartmann, A., Bifulco, C., et al. (2014). Towards the introduction of the 'Immunoscore' in the classification of malignant tumours. J. Pathol. *232*, 199–209.

Grupp, S.A., Kalos, M., Barrett, D., Aplenc, R., Porter, D.L., Rheingold, S.R., Teachey, D.T., Chew, A., Hauck, B., Wright, J.F., et al. (2013). Chimeric antigen receptor-modified T cells for acute lymphoid leukemia. N. Engl. J. Med. *368*, 1509–1518.

Gryfe, R., Kim, H., Hsieh, E.T., Aronson, M.D., Holowaty, E.J., Bull, S.B., Redston, M., and Gallinger, S. (2000). Tumor microsatellite instability and clinical outcome in young patients with colorectal cancer. N. Engl. J. Med. *342*, 69–77.

Gubin, M.M., Zhang, X., Schuster, H., Caron, E., Ward, J.P., Noguchi, T., Ivanova, Y., Hundal, J., Arthur, C.D., Krebber, W.J., et al. (2014). Checkpoint blockade cancer immunotherapy targets tumour-specific mutant antigens. Nature *515*, 577–581.

Hodi, F.S., O'Day, S.J., McDermott, D.F., Weber, R.W., Sosman, J.A., Haanen, J.B., Gonzalez, R., Robert, C., Schadendorf, D., Hassel, J.C., et al. (2010). Improved survival with ipilimumab in patients with metastatic melanoma. N. Engl. J. Med. *363*, 711–723.

June, C.H. (2007). Principles of adoptive T cell cancer therapy. J. Clin. Invest. *117*, 1204–1212.

Le, D.T., Uram, J.N., Wang, H., Bartlett, B.R., Kemberling, H., Eyring, A.D., Skora, A.D., Luber, B.S., Azad, N.S., Laheru, D., et al. (2015). PD-1 Blockade in Tumors with Mismatch-Repair Deficiency. N. Engl. J. Med. *372*, 2509–2520.

Llosa, N.J., Cruise, M., Tam, A., Wicks, E.C., Hechenbleikner, E.M., Taube, J.M., Blosser, R.L., Fan, H., Wang, H., Luber, B.S., et al. (2015). The vigorous immune microenvironment of microsatellite instable colon cancer is balanced by multiple counter-inhibitory checkpoints. Cancer Discov. *5*, 43–51.

Locker, G.Y., Hamilton, S., Harris, J., Jessup, J.M., Kemeny, N., Macdonald, J.S., Somerfield, M.R., Hayes, D.F., and Bast, R.C., Jr.; ASCO (2006). ASCO 2006 update of recommendations for the use of tumor markers in gastrointestinal cancer. J. Clin. Oncol. *24*, 5313–5327.

Mlecnik, B., Tosolini, M., Kirilovsky, A., Berger, A., Bindea, G., Meatchi, T., Bruneval, P., Trajanoski, Z., Fridman, W.H., Pagès, F., and Galon, J. (2011). Histopathologic-based prognostic factors of colorectal cancers are associated with the state of the local immune reaction. J. Clin. Oncol. *29*, 610–618.

Mlecnik, B., Bindea, G., Angell, H.K., Sasso, M.S., Obenauf, A.C., Fredriksen, T., Lafontaine, L., Bilocq, A.M., Kirilovsky, A., Tosolini, M., et al. (2014). Functional network pipeline reveals genetic determinants associated with in situ lymphocyte proliferation and survival of cancer patients. Sci. Transl. Med. *6*, 228ra37.

Nagtegaal, I.D., Quirke, P., and Schmoll, H.J. (2012). Has the new TNM classification for colorectal cancer improved care? Nat. Rev. Clin. Oncol. *9*, 119–123.

Nosho, K., Baba, Y., Tanaka, N., Shima, K., Hayashi, M., Meyerhardt, J.A., Giovannucci, E., Dranoff, G., Fuchs, C.S., and Ogino, S. (2010). Tumour-infiltrating T-cell subsets, molecular changes in colorectal cancer, and prognosis: cohort study and literature review. J. Pathol. *222*, 350–366.

Ogino, S., Nosho, K., Irahara, N., Meyerhardt, J.A., Baba, Y., Shima, K., Glickman, J.N., Ferrone, C.R., Mino-Kenudson, M., Tanaka, N., et al. (2009). Lymphocytic reaction to colorectal cancer is associated with longer survival, independent of lymph node count, microsatellite instability, and CpG island methylator phenotype. Clin. Cancer Res. *15*, 6412–6420.

Ogino, S., Galon, J., Fuchs, C.S., and Dranoff, G. (2011). Cancer immunology–analysis of host and tumor factors for personalized medicine. Nat. Rev. Clin. Oncol. *8*, 711–719.

Pagès, F., Berger, A., Camus, M., Sanchez-Cabo, F., Costes, A., Molidor, R., Mlecnik, B., Kirilovsky, A., Nilsson, M., Damotte, D., et al. (2005). Effector memory T cells, early metastasis, and survival in colorectal cancer. N. Engl. J. Med. *353*, 2654–2666.

Pagès, F., Kirilovsky, A., Mlecnik, B., Asslaber, M., Tosolini, M., Bindea, G., Lagorce, C., Wind, P., Marliot, F., Bruneval, P., et al. (2009). In situ cytotoxic and memory T cells predict outcome in patients with early-stage colorectal cancer. J. Clin. Oncol. *27*, 5944–5951.

Pardoll, D.M. (2012). The blockade of immune checkpoints in cancer immunotherapy. Nat. Rev. Cancer *12*, 252–264.

Popat, S., Hubner, R., and Houlston, R.S. (2005). Systematic review of microsatellite instability and colorectal cancer prognosis. J. Clin. Oncol. *23*, 609–618.

Restifo, N.P., Dudley, M.E., and Rosenberg, S.A. (2012). Adoptive immunotherapy for cancer: harnessing the T cell response. Nat. Rev. Immunol. *12*, 269–281.

Ribic, C.M., Sargent, D.J., Moore, M.J., Thibodeau, S.N., French, A.J., Goldberg, R.M., Hamilton, S.R., Laurent-Puig, P., Gryfe, R., Shepherd, L.E., et al. (2003). Tumor microsatellite-instability status as a predictor of benefit from fluorouracil-based adjuvant chemotherapy for colon cancer. N. Engl. J. Med. *349*, 247–257.

Robert, C., Thomas, L., Bondarenko, I., O'Day, S., Weber, J., Garbe, C., Lebbe, C., Baurain, J.F., Testori, A., Grob, J.J., et al. (2011). Ipilimumab plus dacarbazine for previously untreated metastatic melanoma. N. Engl. J. Med. *364*, 2517–2526.

Rooney, M.S., Shukla, S.A., Wu, C.J., Getz, G., and Hacohen, N. (2015). Molecular and genetic properties of tumors associated with local immune cytolytic activity. Cell *160*, 48–61.

Schumacher, T.N., and Schreiber, R.D. (2015). Neoantigens in cancer immunotherapy. Science *348*, 69–74.

Schumacher, T., Bunse, L., Pusch, S., Sahm, F., Wiestler, B., Quandt, J., Menn, O., Osswald, M., Oezen, I., Ott, M., et al. (2014). A vaccine targeting mutant IDH1 induces antitumour immunity. Nature *512*, 324–327.

Shannon, P., Markiel, A., Ozier, O., Baliga, N.S., Wang, J.T., Ramage, D., Amin, N., Schwikowski, B., and Ideker, T. (2003). Cytoscape: a software environment for integrated models of biomolecular interaction networks. Genome Res. *13*, 2498–2504.

Snyder, A., Makarov, V., Merghoub, T., Yuan, J., Zaretsky, J.M., Desrichard, A., Walsh, L.A., Postow, M.A., Wong, P., Ho, T.S., et al. (2014). Genetic basis for clinical response to CTLA-4 blockade in melanoma. N. Engl. J. Med. *371*, 2189–2199.

Sobin, L., and Wittekind, C. (2002). TNM classification of malignant tumors (New York: Wiley-Liss).

Spranger, S., Bao, R., and Gajewski, T.F. (2015). Melanoma-intrinsic β-catenin signalling prevents anti-tumour immunity. Nature *523*, 231–235.

Topalian, S.L., Hodi, F.S., Brahmer, J.R., Gettinger, S.N., Smith, D.C., McDermott, D.F., Powderly, J.D., Carvajal, R.D., Sosman, J.A., Atkins, M.B., et al. (2012). Safety, activity, and immune correlates of anti-PD-1 antibody in cancer. N. Engl. J. Med. *366*, 2443–2454.

Tosolini, M., Kirilovsky, A., Mlecnik, B., Fredriksen, T., Mauger, S., Bindea, G., Berger, A., Bruneval, P., Fridman, W.H., Pagès, F., and Galon, J. (2011). Clinical impact of different classes of infiltrating T cytotoxic and helper cells (Th1, th2, treg, th17) in patients with colorectal cancer. Cancer Res. *71*, 1263–1271.

Tougeron, D., Maby, P., Elie, N., Fauquembergue, E., Le Pessot, F., Cornic, M., Sabourin, J.C., Michel, P., Frébourg, T., and Latouche, J.B. (2013). Regulatory T lymphocytes are associated with less aggressive histologic features in microsatellite-unstable colorectal cancers. PLoS ONE *8*, e61001.

Trautmann, K., Terdiman, J.P., French, A.J., Roydasgupta, R., Sein, N., Kakar, S., Fridlyand, J., Snijders, A.M., Albertson, D.G., Thibodeau, S.N., and Waldman, F.M. (2006). Chromosomal instability in microsatellite-unstable and stable colon cancer. Clin. Cancer Res. *12*, 6379–6385.

Vacchelli, E., Galluzzi, L., Fridman, W.H., Galon, J., Sautès-Fridman, C., Tartour, E., and Kroemer, G. (2012). Trial watch: Chemotherapy with immunogenic cell death inducers. OncoImmunology *1*, 179–188.

Weitz, J., Koch, M., Debus, J., Höhler, T., Galle, P.R., and Büchler, M.W. (2005). Colorectal cancer. Lancet *365*, 153–165.

Westra, J.L., Plukker, J.T., Buys, C.H., and Hofstra, R.M. (2004). Genetic alterations in locally advanced stage II/III colon cancer: a search for prognostic markers. Clin. Colorectal Cancer *4*, 252–259.

Williams, D.S., Bird, M.J., Jorissen, R.N., Yu, Y.L., Walker, F., Zhang, H.H., Nice, E.C., and Burgess, A.W. (2010). Nonsense mediated decay resistant mutations are a source of expressed mutant proteins in colon cancer cell lines with microsatellite instability. PLoS ONE *5*, e16012.

Zlobec, I., Karamitopoulou, E., Terracciano, L., Piscuoglio, S., Iezzi, G., Muraro, M.G., Spagnoli, G., Baker, K., Tzankov, A., and Lugli, A. (2010). TIA-1 cytotoxic granule-associated RNA binding protein improves the prognostic performance of CD8 in mismatch repair-proficient colorectal cancer. PLoS ONE *5*, e14282.